SHOCK STAGE ASSESSMENT AND PETROGRAPHY OF 11 ANTARCTIC ENSTATITE CHONDRITES

M. R. M. Izawa[1*], R. L. Flemming[1], N. R. Banerjee[1]
[1]Department of Earth Sciences, The University of Western Ontario, 1151 Richmond St., London, ON, Canada N6A5B7 *matthew.izawa@gmail.com

Introduction: Meteorites are delivered to Earth by ejection from a parent body during hypervelocity impact events. Many meteorites, especially chondrites, originate in asteroid regolith breccias, and have experienced multiple shock events. An understanding of shock metamorphic effects in chondritic meteorites is therefore critical to disentangling the signatures of nebular, parent body, and terrestrial processes.

Enstatite (E) chondrites have formed under anhydrous, highly reducing conditions which are fundamentally different from those experienced by ordinary and carbonaceous chondrites [1]. They are thought to originate from parent objects that formed near the proto-sun.

Assigning shock stages to enstatite chondrites is challenging, because: 1) most lack olivine; 2) large grains of plagioclase are rare in all but the most equilibrated samples; and 3) silicate darkening due to minute metal/sulfide inclusions reduces the ability to distinguish petrographic shock indicators such as twinning, exsolution, amorphization and planar fractures/planar deformation features. Enstatite chondrites also weather rapidly under terrestrial conditions; therefore silicates are often stained by Fe-oxyhydroxides, which may further obscure petrographic shock indicators. The indicators of shock stage in orthopyroxene for ordinary and enstatite chondrites have been described by [2].

Shock induced lattice deformation is known to induce asterism or 'streakiness' in single-crystal XRD patterns [3, 4]. This asterism is interpreted as representing mosaicity in the crystal lattice [3, 4, 5]. This study applies the micro X-ray diffraction technique (μXRD) to compliment petrographic assessments of shock level for eleven enstatite chondrites. Five of these have previously been assigned shock stages by [2], though the sections used here were used in this previous work. Heterogeneity in the meteorites may play a role in creating discrepancies between these two studies. It is important to note that many investigators have found that the apparent degree of shock expressed in minerals in impact breccias is often highly varied [e.g. 6-10]. As many of these meteorites are likely to have originated in asteroid regolith breccias, it is likely that they are also subject to such variations.

Methods and Samples: Polished thin sections of EH and EL chondrites from a complete range of thermal metamorphic grades were investigated with a petrographic microscope in transmitted and reflected light. Following the method of [11], shock stage is determined by the highest stage indicated by at least 25% of the grains investigated. Shock stage assignment was made using the shock features in orthopyroxene described by [2]. All samples are Antarctic finds, sample identities; types and thin section numbers are summarized in Table 1. Areas of particular interest were selected for μXRD analysis. Micro XRD data were collected using the Bruker AXS D8 Discover micro X-ray diffractometer at the University of Western Ontario, using Cu Kα radiation (λ = 1.54441 Å) with a 500 μm beam diameter. A two-dimensional General Area Diffraction Detector System (GADDS) collects the diffracted X-rays. For further details of the μXRD apparatus and technique, see [10]. Analysis of the distribution of intensity along the Debye rings in the GADDS images allows determination of textural/microstructural information including shock-induced asterism. Intensity of the diffracted rays was integrated along the Debye rings to produce plots of intensity vs. χ, the angle subtended by the Debye rings. To ensure that the mosaicity is related to orthopyroxene and not to other phases (especially metal and sulfides, which can be highly deformed in the process of thin section preparation) the peaks integrated for intensity vs. χ plots were chosen so as to avoid overlap with peaks from other minerals. The (020), (610) and (131) reflections were chosen. As the normal vectors to these planes constitute a basis for three-dimensional space, this allows, in principle, for the assessment of the strain in any crystallographic direction.

Results: The shock stages of these meteorites and other petrographic observations are summarized in Table 1. For peaks (020), (610) and (131), the average full width at half maximum (FWHM) integrated along χ was determined for each sample. Only peaks with intensity >2 standard deviations above noise were used in this analysis. There is a clear correlation between moscaicity inferred from μXRD and petrographic shock stage (see Fig. 1). Enstatite grains in many of these meteorites contain abundant inclusions, with morphologies ranging from rounded spheroids ~few microns in diameter to elongate needles up to ~tens of microns in length interpreted as melt inclusions. These are distinct from the metal-sulphide inclusions related to silicate darkening: they are not opaque; commonly exhibit elongated habits, and appear to have crystallographically-controlled boundaries. These inclusions commonly occur along planar and

irregular fractures, and may preserve a record of such fractures through thermal annealing.

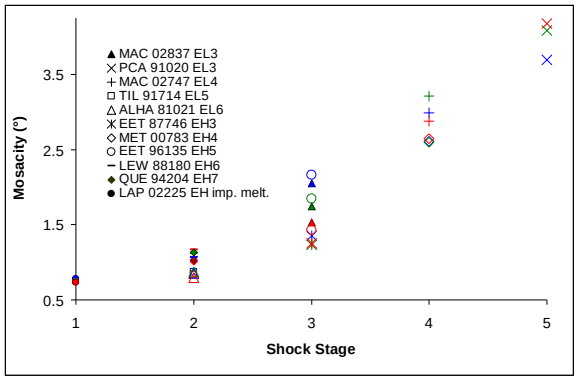

Figure 1: Mosaicity vs. shock stage. Blue symbols: (020) reflections; Green: (610); Red (131). There is a direct correlation between mosaicity and petrographic shock stage. There are no systematic variations in mosaicity between these lattice planes.

Discussion: There is a general increase in mosaicity in diffraction peaks and petrographic shock stage (see Fig. 1). There is no systematic variation in mosaicity between different lattice planes. Silicate darkening due to minute metal and/or sulphide inclusions is apparent in most of these meteorites, see Table 1. As many effects beyond shock, including thermal metamorphism, *in situ* reduction of nebular FeO and weathering can lead to silicate darkening, there is no strong correlation between shock stage and the degree of silicate darkening [11, 12]. Type 5 and 6 E chondrites, and E chondrite melt rocks, are of lower shock stage than types 3 and 4. However, many of the higher thermal metamorphic grade E chondrites show evidence of thermal annealing from higher shock stages, such as the preservation of relict clinopyroxene lamellae or twin boundaries by metal-sulfide intrusions.

Conclusions: Shock stages as determined by optical petrography in this study are in good agreement with previous work. It is suggested that intra-sample heterogeneity may account for the discrepancy in the case of LEW 88180. Mosaicity as inferred from μXRD data shows a general increase with increasing petrographic shock stage. There are no systematic differences in mosaicity of the (020), (610) and (131) reflections of orthopyroxene, implying that lattice strain is distributed isotropically. Micro XRD shows promise as an independent means of assessing shock stage in chondritic meteorites, in both thin sections and intact samples, and may be of particular value when dealing with very small grains, silicate darkening, weathering/staining and other effects, which obscure the usual petrographic indicators of shock.

Meteorite	MAC 02837	PCA 91020	MAC 02747	TIL 91714	ALHA 81021	EET 87746	MET 00783	EET 96135	LEW 88180	QUE 94204	LAP 02225
Type	EL 3	EL 3	EL 4	EL 5	EL 6	EH 3	EH 4	EH 5	EH 6	EH 7	EH imp. melt
Weathering Grade	C	Ce	B/C	C	A-C	Ce	C	B	C/Ce	C	B
Shock Stage, this study	S3	S5	S4	S2	S2	S3	S4	S3	S2†	S2	S1
Thin Section #, this study	16	43	8	3	44	4	6	6	9	26	9
Shock Stage [2]	N/A	S5	N/A	S2	S2	S3	N/A	N/A	S3*	S2	N/A
Thin Section # [2]	N/A	19	N/A	9	46	32	N/A	N/A	19	10	N/A
Silicate Darkening	Mod.	High	Low	High	Low	Mod.	Low	High	High	Low	Low
Melt Inclusions	Mod.	Low	High	High	Low	Mod.	High	Low	Low	High	High

*[2] classified LEW 88180 as an EH5 †Probably S3-4 which reverted/annealed

Table 1: Summary of the mineralogy and petrology of the 11 E chondrites in this study, some data from [2].

References: [1] Brearley A. J. & Jones R. H. (1998) Chondritic Meteorites. In *Planetary Materials* (ed. J. J. Papike), pp. 398. Min. Soc. Amer., Washington, D.C. [2] Rubin A. E., Scott E. R. D., & Keil K. (1997). *GCA* **61** (4), 847-858. [3] Hörz F. & Quaide W. L. (1973) *The Moon* **6** (1-2), 45-86. [4] Flemming R. L. (2007). *Can. J. Earth Sciences* **44**, 1333-1346. [5] Flemming, R. L. McCaulsland, P. J. A., Izawa, M. R. M. and Jacques, N. (2007). *38th LPSC* #2363. [6] French B. M. (1998) *Traces of Catastrophe:* pp. 61-78. LPI, Houston, TX. [7] Keil K. (1989). *Meteoritics* **24**, 195-208. [8] Osinski G. R., Spray J. G., & Lee P. (2005) *MAPS* **40** (12), 1789-1812. [9]. Redeker H. J. & Stöffler D. (1988) *Meteoritics* **23** (3), 185-196. [10] Stoffler D. & Ostertag R. (1983) The Ries Impact Crater. *For. D. Min.* **61** (2), 71-116. [11] Stöffler D., Keil K., & Scott E. R. D. (1991) *GCA* **55** (12), 3845-3867. [12] Rubin A. E. (1997). *MAPS* **32**, 231-247.